Chemical *in situ* modulation of doping interactions between oligoanilines and nanocarbon films

Enamul Hoque, Tanzina Chowdhury, Peter Kruse*

Department of Chemistry and Chemical Biology, McMaster University,

1280 Main Street West, Hamilton, Ontario, L8S 4M1, Canada

* Author to whom correspondence should be addressed, email: pkruse@mcmaster.ca

Keywords: Interfacial Doping; Oligoaniline; Polyaniline; Carbon Nanotubes; Raman; Chemiresistive Sensors

Abstract

This paper is dedicated to Professor P.R. Norton on the occasion of his 75th birthday, in honor of his profound contributions to Surface Science.

The electronic properties of carbon nanotubes are commonly customized through doping with various moieties, however, the modification is permanent as long as the dopant is present. Here we present a family of dopants that can be switched on and off while in place via environmental stimuli, in particular redox conditions and exposure to acids and bases. Aniline oligomers are firmly attached to the carbon nanotubes and are not easily displaced by other dopants or through rinsing with solvent in either oxidation state. As opposed to the reduced form of the aniline oligomers, their oxidized form causes p-doping of the carbon nanotubes. Similarly, the free base and chloride salt form of the aniline oligomers can be distinguished by their doping impact on the carbon nanotubes. The switching of the doping state can be followed by X-ray photoelectron spectroscopy, Raman spectroscopy and especially also electrically (film resistance), opening up applications as switches and sensors.

1. Introduction

Many applications of single-walled carbon nanotubes (SWCNTs) rely on our ability to customize their electronic properties [1,2,3]. Carbon nanotubes can be used as circuit elements, solar cells, switches or sensors [4-9]. Particularly in sensing applications, for carbon nanotubes to work as transducers they have to vary their electronic properties in response to environmental stimuli, e. g. of mechanical, thermal, electromagnetic or chemical nature. Most chemical sensors require amplification due to the marginal change in electronic properties as a function of a small change in the magnitude of a stimulus that is nevertheless desirable to detect. Amplification strategies include sophisticated control electronics, nanostructured percolation conductivity networks [10,11], as well as chemical field effect transistors (ChemFETs) [12]. SWCNT-based sensors have the potential to circumvent the need for additional amplification, because certain select analytes (e.g. ammonia [8]) cause a strong change in the SWCNT electronic structure ("doping") and can be detected very sensitively by simple resistance measurement of a SWCNT film [13].

The process of modifying the electronic structure of SWCNTs by removing or adding charge is known as 'doping'. Permanent doping of carbon nanotubes can be achieved either by substitutional or by chemical doping. Substitutional doping involves replacing some carbon atoms in the SWCNT structure with atoms that have a different number of valence electrons, such as boron (p-doping) or nitrogen (n-doping) [14], and is not of concern to us here. The electronic structure of SWCNTs can also be modulated via chemical doping, i.e. the covalent or non-covalent attachment of functional groups or molecules that withdraw (p-doping) or donate (n-doping) charge to the SWCNT host [15,16]. Numerous molecules have been identified which induce charge transfer from (e.g. molecular oxygen [17], $FeCl_3$ [18], TCNQ [19,20], $TCNQF_4$ [19,20,21]) or to (e.g. ammonia [8], alkylamines [22,23], alkali metals [24], TTF [19,20], TDAE [19,20]) SWCNTs.

Furthermore, the charge carrier density can also be modulated by applied external electric fields (e.g. in field effect transistors) [7], which has the benefit that the doping state of the SWCNTs can be changed over time, unlike in the case of traditional chemical dopants. It would be desirable to modulate the effect of chemical dopants directly by environmental stimuli, such as light [25] or chemical environment [26-28].

Aniline oligomers and polyanilines (PANI) are an interesting class of molecules that have been reported to interact with carbon nanotubes electronically [29,30]. Carbon nanotubes have been reported to act as dopants for PANI films [13,31]. PANI and its oligomers are also known for being able to assume different oxidation states [32-34]. The impact of a change in oxidation state of PANI or one of its oligomers on its ability to dope SWCNTs has never been documented or utilized, however. Only on one occasion it has been mentioned that PANI can be used to control doping in carbon nanotube devices [7].

Here we introduce aniline oligomers as a class of switchable dopants for carbon nanotubes. We are elucidating the interactions of the phenyl-capped aniline dimer (diphenyl p-phenylenediamine, DPPD) and phenyl-capped aniline tetramer (PCAT) with SWCNTs using UV-visible spectroscopy, Raman spectroscopy, X-ray photoelectron spectroscopy (XPS), and electrical resistance measurements. In the oxidized state(s), the oligomers strongly p-dope SWCNTs, while the fully reduced state does not result in any detectable doping effect. Hence films of aniline oligomer doped carbon nanotubes are suitable candidates for redox-sensors, since their electrical resistivity strongly depends on their doping state and hence the redox state of the aniline oligomers, which in turn depends sensitively on the chemical environment of the films.

2. Experimental

SWCNTs (Unidym, formerly Carbon Nanotechnologies Inc., HiPco process, batch# PO343) were annealed at 800°C under vacuum for 1 hour (after ramping up at 1°C/min) to remove any residual contaminants [35,36]. Phenyl-capped aniline dimer (diphenyl p-phenylenediamine, DPPD) was purchased from Sigma Aldrich. Phenyl-capped aniline tetramer (PCAT) was synthesized and purified according to published procedures [34,37]. Both oligomers were converted into the desired oxidations states before use as described below. Ammonium persulphate (98.0% pure, Sigma Aldrich), L-ascorbic acid (99.0% pure, Caledon), hydrochloric acid (LabChem, Inc.), potassium hydroxide (Fisher Scientific) and methanol (anhydrous, Comalc) were used as received. PTFE 0.2 µm filter membrane was purchased from Pall Life Science.

SWCNTs were mixed with the dopant molecules (DPPD or PCAT) while maintaining the SWCNT to dopant mass ratios constant throughout the study. Methanol was used as a solvent for all experiments. SWCNTs were also suspended in methanol as a reference sample. The weight to volume ratio for SWCNT samples suspended in methanol was maintained throughout the study. Batches of DPPD and PCAT were dissolved in methanol and combined with either ammonium persulfate as an oxidizing reagent or ascorbic acid as a reducing agent in slight stoichiometric excess in order to obtain their fully oxidized or reduced forms respectively [32]. The half-oxidized form of PCAT was obtained from the fully reduced form by mixing it with the appropriate stoichiometric amount of the oxidizing reagent. Sonication of all samples prepared with SWCNTs and oligomers was performed under ambient conditions for 1 hour in a Branson 1510 bath sonicator (42 kHz, 70 W). The respective samples of oligomers mixed with oxidizing agent, reducing agent, acid or base were sonicated for 5 to 10 minutes. The suspensions were dropped on glass slides and dried in air, or filtered through PTFE membranes to prepare bucky-paper-style

samples for Raman spectroscopy. Flakes of the bucky paper obtained from filtered samples were collected on glass slides for Raman spectroscopy.

Raman spectra were recorded with a Renishaw 2000 Raman microscope over a range of 100 – 3600 cm^{-1}, with a spectral resolution of 2 cm^{-1}, using a 50× objective in backscattering configuration. Data were collected on several spots on the samples having a size of about 1.2 µm and recorded with a fully focused 514 nm laser at 1% power, corresponding to a power density of ~ 10 $\mu W/\mu m^2$ in order to avoid laser damage to the sample [38]. Where explicitly mentioned, some Raman spectra were collected using a 785 nm solid state laser. The spectra were scaled with respect to the maximum intensity of the D* mode (2570 - 2730 cm^{-1}) to visually aid the comparison within and amongst the samples [39]. The D* peaks have been de-convoluted by Lorenztian peak fitting. UV-vis spectra were recorded on an Ultrospec™ 100 *pro* Visible Spectrophotometer with a wavelength range of 330 - 830 nm, a spectral band width of 8 nm and a wavelength accuracy of ±2 nm. Before recording each UV-vis spectrum of an oligomer, the spectrometer was calibrated with methanol. Powder samples of reduced PCAT, oxidized PCAT, half-oxidized PCAT, reduced PCAT mixed with SWCNTs, oxidized PCAT mixed with SWCNTs, and half-oxidized PCAT mixed with SWCNTs were pressed into double-sided adhesive tape and analyzed by X-ray photoelectron spectroscopy (XPS) using a Kratos Axis Ultra X-ray photoelectron spectrometer. High resolution analyses were carried out with an analysis area of 300 x 700 μm^2 and a pass energy of 20 eV.

For electrical characterization, a SWCNT film was drop-casted from a methanolic suspension between two gold electrodes on a substrate, and then covered by a microfluidic channel such that any liquid flown through the channel could not contact the gold electrodes directly. A methanolic solution of DPPD was then flown over the SWCNT film, followed by a pure methanol rinse and

methanolic solutions of the oxidizing and reducing reagents respectively. Resistance of the film was measured by applying a 0.1 mV potential and measuring the current response in a simple two electrode configuration. Several devices were tested to assure reproducibility.

3. Results and discussion

3.1. Oxidized aniline oligomers p-dope SWCNTs

Different oxidation states of DPPD and PCAT were produced, and their effect on SWCNTs was studied using Raman spectroscopy. (Fig. 1) DPPD is an aniline dimer that is terminated with an additional phenyl ring, whereas PCAT is an aniline tetramer that is also terminated with an additional phenyl ring. Even-numbered aniline oligomers have the special property that pairs of neighboring amine groups can lose their attached hydrogen atoms, in effect oxidizing the molecule [32]. These oxidized versions of the aniline oligomers can then add pairs of hydrogen atoms to neighboring imine groups to regenerate the amine groups of the reduced molecules. Raman spectra of predominantly semiconducting SWCNTs interacting with reduced (amine, Figs. 1a) and oxidized (imine, Fig. 1b) PCAT molecules were taken with a 514 nm green laser [40], and contrasted with spectra taken on the same sample with a 785 nm red laser that preferentially excites metallic SWCNTs (Figs. 1c, d). All typical Raman features of SWCNTs are present: radial breathing modes between 100 and 300 cm^{-1}, the G-band around 1590 cm^{-1}, and the D^{*}-band around 2660 cm^{-1} [35,36,38]. Since the Raman spectral features of carbon nanotubes are resonantly enhanced, the PCAT molecular features in a mixed sample are not normally visible. For the purpose of Figure 1 only, a large excess of PCAT was used, so that some features of the molecules are also visible in the spectra, namely the bands at 1179, 1221 and 1621 cm^{-1} typical of reduced PCAT in Fig. 1a and the bands at 1166, 1218 and 1498 cm^{-1} typical of oxidized PCAT in Fig. 1b

[41,42]. Some molecular features overlap with the G band of the SWCNTs, but for the interaction with oxidized molecules a blue shift of 10 cm^{-1} is seen in the location of the D*-band of the semiconducting nanotubes. The 785 nm laser is not well-suited for detection of the molecular features, but it can be seen that the oxidized PCAT molecules had a significant impact on the metallic nanotubes, as witnessed by the rise of a very large D peak at 1370 cm^{-1} (Fig. 1d) while the D* feature has almost vanished.

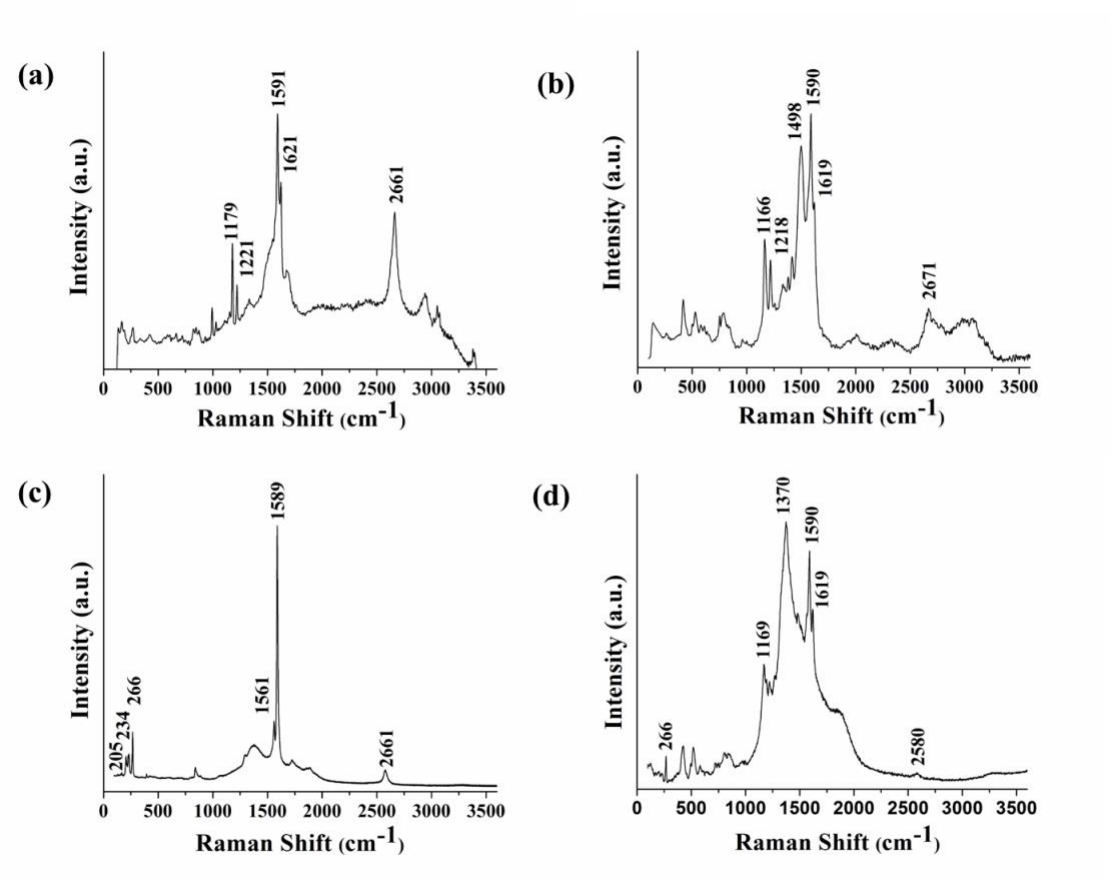

Fig. 1. Raman spectra of SWCNT's mixed with PCAT. (a) SWCNTs mixed with reduced PCAT illuminated by a 514 nm laser, (b) SWCNTs mixed with oxidized PCAT illuminated by a 514 nm laser, (c) SWCNTs mixed with reduced PCAT illuminated by a 785 nm laser, (d) SWCNTs mixed with oxidized PCAT illuminated by a 785 nm laser.

For the remainder of the work, Raman spectra of molecule - SWCNT complexes were taken with a 514 nm laser over a range from 100 to 3600 cm^{-1}, but for clarity only the D* feature at around 2660 cm^{-1} is presented in the following figures, since a shift in the location of this peak is sufficiently indicative of the SWCNT doping state [35,43]. When Raman spectra of freshly annealed SWCNT networks were taken after 30 min sonication in pure methanol, the main peak of the D* feature is located at 2656 cm^{-1}. (Fig. 2a, also see Fig. S1 in Supporting Materials for a full spectrum) This position is typical for un-doped SWCNT films [35,36]. Methanol - as a radical quencher - was used in this study instead of water in order to avoid doping effects due to O_2 species from water sonication [36]. It is also a reasonably good solvent for our dopant molecules, thus providing for homogeneous samples of strongly attached molecules rather than non-interacting mixtures of molecules and SWCNTs.

When the reduced form of DPPD was added to SWCNT samples in methanol, the position of the main peak of the D* feature essentially remains the same as for the pure SWCNT sample. (not shown) While reduced DPPD should be expected to n-dope carbon nanotubes [7], we were unable to distinguish the presumably weakly n-doped state of the SWCNTs from the undoped state. This is likely because the reduced form of DPPD is not planar [44,45], and interactions between the amine and the SWCNTs are therefore sterically inhibited. In the case of a long polymer chain, there will be a better chance of random interaction of some of the amine groups with the SWCNTs [7]. A bucky paper film of this sample was formed on a filter paper, and rinsed with a methanolic solution of a suitable oxidant, namely ammonium persulfate as previously reported in the literature [32]. The Raman spectrum of a sample of the resulting film indeed shows a blue-shift of 8 cm^{-1} in the D* peak, indicative of p-doping. (Fig. 2b) That in itself cannot be taken as ultimate proof that the oxidized form of DPPD is a p-dopant, considering that a reaction product of the oxidation of

DPPD with persulfate is sulfate, which itself has been shown to have a strong p-doping effect [36]. Indeed, a bare SWCNT film produced in a similar manner to the DPPD-SWCNT film and exposed to a methanolic solution of ammonium persulfate also shows a blueshift, even stronger so at 13 cm^{-1}. (Fig. 2c) This shift is to be expected for sulfate ions [36]. A clear distinction between the two cases becomes possibly after rinsing with a methanolic solution of ascorbic acid, which acts as a reducing agent in the case of the DPPD, and resets the DPPD-SWCNT films into the original state. (Fig. 2d) No impact is made on the sulfate-doped SWCNT films. (Fig. 2e) Hence we can conclude that DPPD is not only capable of being switched between p-doping and not-doping states while being attached to SWCNT films, but it also prevents the interaction of other dopants (namely sulfate) with the SWCNTs due to the formation of a continuous (mono)layer [46-48].

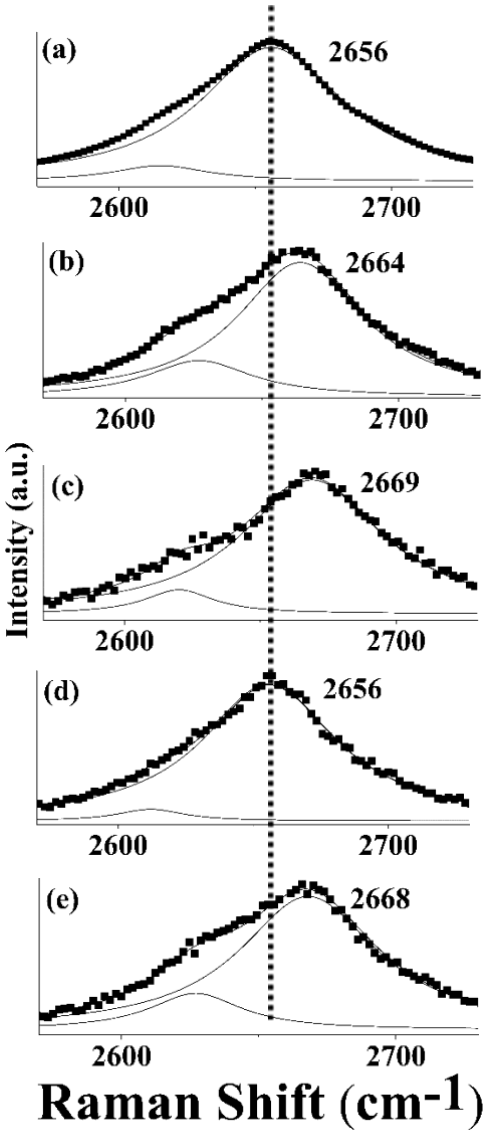

Fig. 2. Raman spectra (D* peak) demonstrating the effect of DPPD on SWCNT films. (a) Annealed, bare SWCNT film, (b) DPPD - SWCNT composite film after exposure to ammonium persulfate, (c) bare SWCNT film after exposure to ammonium persulfate, (d) DPPD - SWCNT composite film after subsequent exposure to ammonium persulfate and ascorbic acid, (e) bare SWCNT film after subsequent exposure to ammonium persulfate and ascorbic acid.

Similarly, when the SWCNTs were sonicated in methanol together with the fully reduced form of PCAT (instead of by themselves, Fig. 3a), their D* features remained essentially unchanged. (Fig.

3c) When sonicated with the half-oxidized (2 amine and 2 imine groups) version of PCAT, their D* features blue-shifted by 5 cm^{-1}, (Fig. 3e) whereas the fully oxidized version of PCAT yielded a blue-shift of 9 cm^{-1}. (Figs. 3b, 3d)

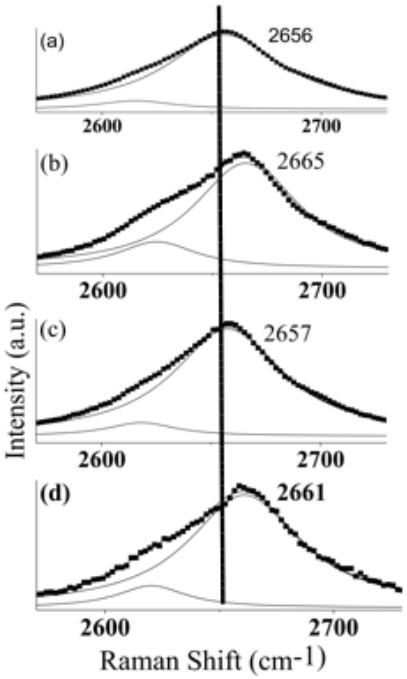

Fig. 3. Raman spectra (D* peak) of SWCNTs demonstrating the doping effects of different PCAT oxidation states. (a) Pristine and annealed SWCNTs sonicated in methanol, (b) SWCNTs with oxidized PCAT, (c) SWCNTs with reduced PCAT, (d) SWCNTs with half-oxidized PCAT.

3.2. The mechanism of doping

Further characterization was carried out in order to elucidate the origin of the switchable doping phenomenon. It is possible to study the Raman spectra of the oligoanilines by themselves, and our spectra (not shown) agree with the literature for the various oxidation states [32,41]. However, we were unable to resolve their Raman features as part of the SWCNT films when used in

stoichiometric ratio, because the resonant signal of the carbon nanotubes by far dominated the spectrum [49]. The spectra shown in Fig. 1 are taken on films with a large excess of PCAT, hence most of the Raman signal comes from molecules that are not directly interacting with the SWCNTs. Here, we present the UV-vis spectra of the oxidized and reduced molecules in pure form in order to highlight their electronic properties, while their impact on the SWCNT films is elucidated using X-ray photoelectron spectroscopy (XPS). The alignment of conduction and valence bands of the SWCNTs with the highest occupied and lowest unoccupied orbitals of the molecules determines magnitude and direction of charge transfer [50]. UV-vis spectra (Fig. 4a) of completely oxidized DPPD species show two absorption bands at 330 nm and 422 nm (upper curve), while the completely reduced DPPD species exhibits only one optical transition at 330 nm (lower curve). The band at 330 nm is associated with a $\pi \rightarrow \pi^*$ type transition of the benzenoid rings, while the band at 422 nm is associated with the presence of quinoid (-N=) rings in the oxidized DPPD species [51]. Thus, the upper curve is characteristic for the oxidized DPPD species. Similarly, the absorbance maximum originating at 330 nm (Fig. 4b) for oxidized and reduced PCAT compounds is ascribed to the π - π^* transition centered on the benzenoid aromatic rings of PCAT species. This is the only type of spectrum expected for the leucoemeraldine (reduced) state of PCAT [37], since it shows essentially no excitonic peak, while more than one transition is expected for oxidized PCAT species. The second absorbance maximum found at 414 nm (upper curve) is due to quinoid rings of the oxidized PCAT species. The third absorbance maximum, observed at 585 nm (upper curve), is indicative of the formation of a molecular exciton qualitatively described by a charge transfer into the quinoid (-N=) rings from each of the neighboring benzenoid rings [52]. The absorbance maximum at 750 - 800 nm (upper curve) has

been attributed to highly delocalized charge carriers [53]. Therefore, this spectrum (upper curve) is characteristic for the pernigraniline (oxidized) base state of PCAT.

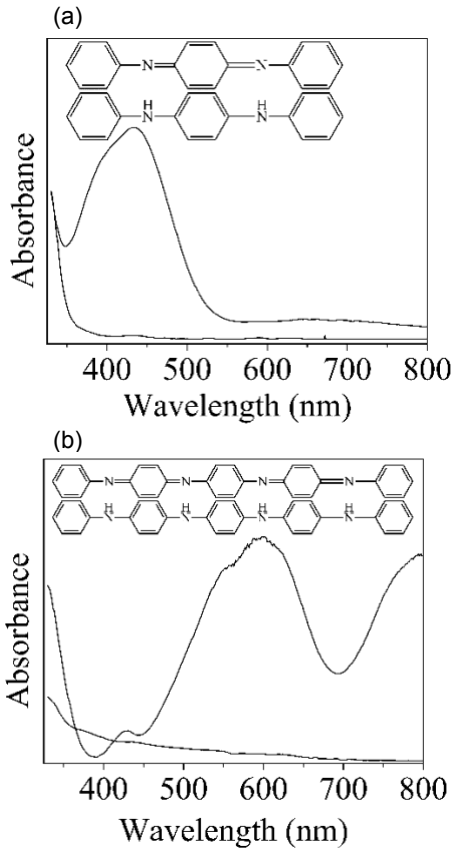

Fig. 4. UV-vis spectra of different oxidation states of the phenyl capped aniline oligomers used in this study. (a) Phenyl-capped aniline dimer (diphenyl p-phenylenediamine, DPPD) in the oxidized (top) and reduced (bottom) form. (b) Phenyl-capped aniline tetramer (PCAT) in the oxidized (top) and reduced (bottom) form.

The impact of the interactions with DPPD and PCAT on the SWCNTs is clearly visible in Figs. 2 and 3 using Raman spectroscopy. However, the impact of those interaction on the molecules cannot be elucidated using Raman or UV-vis spectroscopy, because the signal from the carbon nanotubes by far overwhelms the signal from the molecular species. Therefore we chose X-ray photoelectron spectroscopy (XPS) in order to observe the interactions. The carbon 1s peak will in

this case also be dominated by the SWCNT signal, which would demonstrate a subtle shift due to doping [35]. This small shift (expected to be less than 0.1 eV) cannot be discerned from our data, since our spectra were charge corrected based on the C 1s peak location. The nitrogen 1s peak, however, will be solely indicative of the effect of the doping process on the aniline oligomers [41]. We have obtained high resolution XPS spectra of the N 1s peak of reduced, oxidized and half-oxidized PCAT species, both in pure form and while interacting with SWCNTs. (Fig. 5)

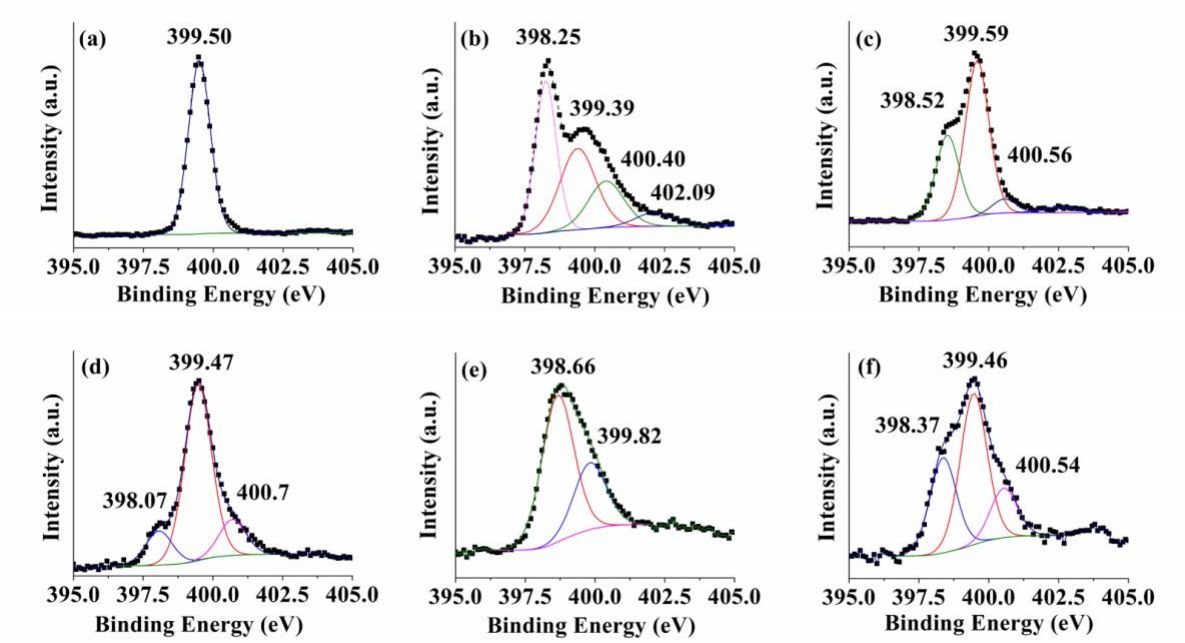

Fig. 5. Nitrogen 1s high resolution XPS spectra (deconvoluted) of (a) reduced PCAT powder, (93.7%) (b) oxidized PCAT powder, (imine 37.9%; amine 34.6%; ox? 19.8%; charged 5.8%) (c) half-oxidized PCAT powder, (31.4%; 57.7%; 5.2%) (d) reduced PCAT mixed with SWCNTs, (13.8%; 71.6%; 14.6%) (e) oxidized PCAT mixed with SWCNTs, (68.7%; 31.3%) (f) half-oxidized PCAT mixed with SWCNTs. (32.2%; 51.1%; 16.8%) Attribution of peaks: ~398.3 eV = imine; ~399.5 eV = amine; ~400.5 = charge at N (protonated); ~402 eV = delocalized charge.

The amine groups of the reduced PCAT molecules manifest themselves in N 1s peak at a binding energy of 399.5 eV, (Fig. 5a) whereas the imine groups of the oxidized molecules result in a N 1s binding energy of 398.25 eV, (Fig. 5b), a clear shift of over 1 eV that makes the two species easily distinguishable [54]. As it can be seen, the 'oxidized' batch of molecules still includes a percentage of reduced species (peak at 399.39 eV), in addition to nitrogen atoms that have lost an electron, but not a proton (peak at 400.40 eV; oxidized, but technically in the salt form rather than the free base), and nitrogen atoms associated with delocalized positive charges (peak at 402.09 eV; still oxidized). Given that 3 of the four peaks are associated with oxidized nitrogen species, the amount of residual reduced PCAT in this sample is estimated to be less than one third. Some reduction may have also occurred due to background hydrogen under irradiation in the XPS vacuum chamber. Finally, the half-oxidized PCAT sample appropriately shows an almost even mix of imine (BE 398.52 eV) and amine (BE 399.59 eV), with only a small amount of protonated nitrogen (BE 400.56 eV) and no discernible delocalized charges (Fig. 5c). The latter is due to the half-oxidized nature of the tetramers, limiting the conjugated system to isolated quinoid rings, rather than pairs of quinoid rings as present in the oxidized tetramers, or even longer conjugated chains in the polymeric form (PANI). Overall, the XPS spectra of the pure PCAT samples are in line with expectations and provide a good reference point for understanding the interactions of these molecules with SWCNTs.

The interaction of reduced PCAT molecules with SWCNTs leads to the emergence of imine and charged nitrogen peaks in the N 1s spectrum (Fig. 5d), both indicative of electron donation from the molecules to the SWCNTs, i.e. n-doping. In the case of oxidized PCAT (Fig. 5e), virtually all charged species have disappeared from the spectrum, while the portion of reduced (amine) N holds steady just below one third. Half-oxidized PCAT contains a mixture of amine and imine moieties,

which upon interaction with SWCNTs individually behave as to be expected from the fully reduced and 'fully' oxidized samples, resulting in a mixture of imine (BE 398.37 eV), amine (BE 399.46 eV) and charged nitrogen (BE 400.54 eV) species (Fig. 5f). This behavior is fully consistent with what we know about carbon nanotube chemistry and physics [55].

3.3. Dopants can be switched on and off repeatedly

To study the reversibility of the doping process due to repeated exposure to oxidizing and reducing agents, SWCNTs were suspended in methanol by sonication for an hour and then formed into a bucky paper style film by filtration onto a PTFE membrane. The Raman spectrum recorded for this sample shows a D* peak at 2656 cm^{-1}, indicating undoped SWCNT networks. (Fig. 6a) The SWCNT film was then rinsed with a methanolic solution of fully oxidized PCAT. This resulted in a 9 cm^{-1} up-shift of the D* peak to 2665 cm^{-1} (Fig. 6b) indicating p-type doping of the SWCNT network. The SWCNT film was then rinsed with a methanolic ascorbic acid solution and the Raman down-shift of the D* peak is found at 2659 cm^{-1}. Fig. 6c illustrates the switching back of the SWCNT networks to the original (un-doped or possibly weakly n-doped) state. Although it does not go all the way back to the D* position (2656 cm^{-1}) of pristine SWCNTs, this recovery effectively constitutes a redox cycle of the SWCNT films and allows the same SWCNT networks to be repeatedly cycled between two stable states via exposure to redox reagents. The stability of the oligoaniline-SWCNT complex is expected, because aromatic structures in general are known to interact strongly with the basal plane of graphitic surfaces via π-stacking [23,31]. The redox recovery cycle has been repeated to confirm its reversibility. The Raman spectrum collected after reducing the SWCNT film one more time with ammonium persulfate reveals again the up-shift of the D* peak to 2665 cm^{-1} (Fig. 6d) and thus p-doping. Subsequent rinsing with ascorbic acid

removed the p-doping effect on the SWCNT film as evidenced by the downshift in the D* peak, (Fig. 6e) which completes the second redox cycle. We have only completed one more cycle (Figs. 6f, 6g), but it can be expected that the system is longterm stable for many more cycles [56,57]. For all the Raman spectroscopy experiments a sample flake was collected on a glass slide after each switching step. As a result, a noticeably large, and nearly identical switching of Raman shift for all the three complete redox reversible cycles has manifested the robust chemical sensing properties of SWCNT networks doped with PCAT species. The nearly identical switching of the Raman shift for all the three redox reversible cycles rules out the possibility of any structural damage to the SWCNT networks in either the oxidized or the reduced state.

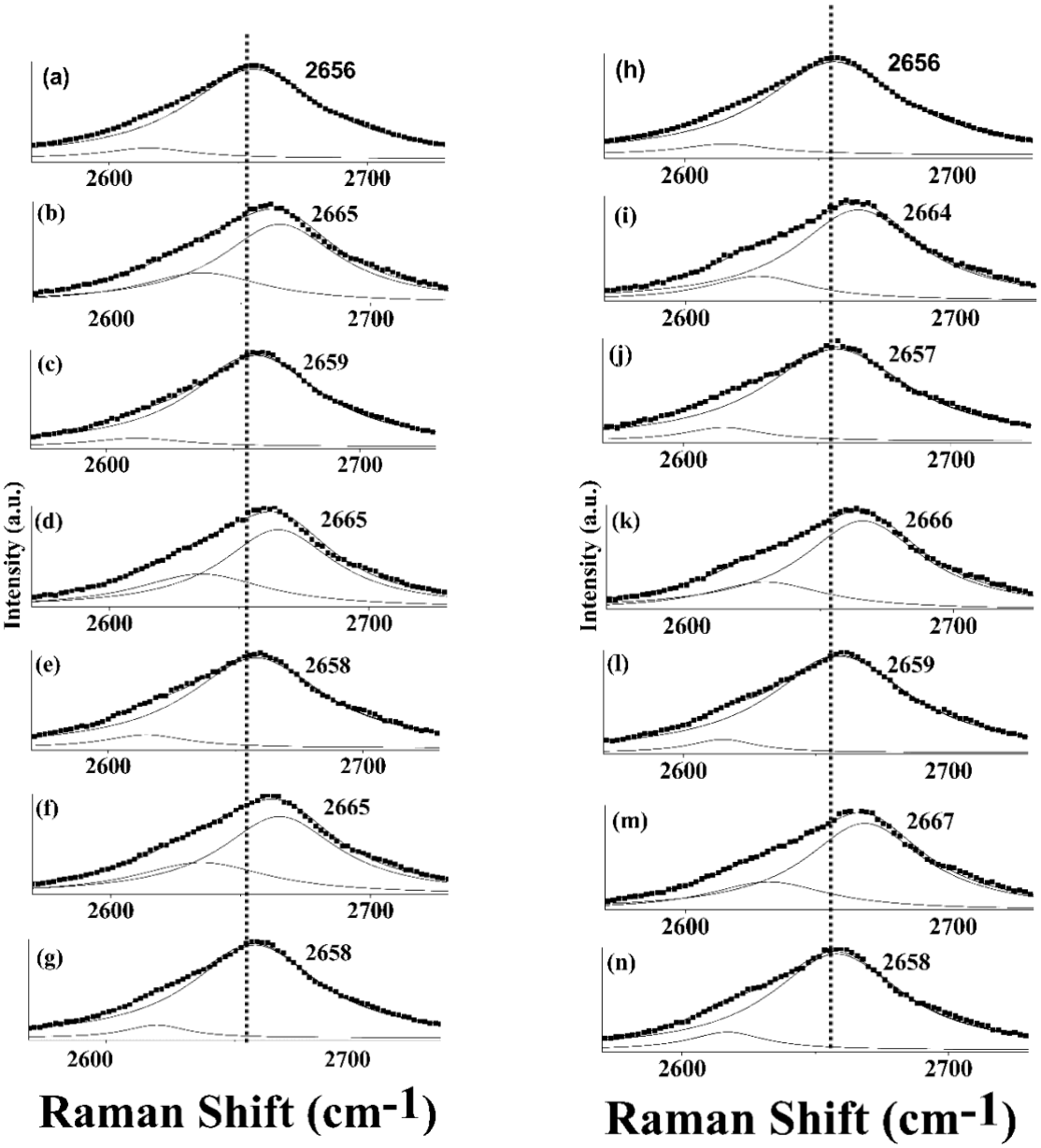

Fig. 6. Raman spectra illustrating the evidence of SWCNTs' switching back and forth between different doping states in response to the oxidized and reduced state of doping species PCAT and DPPD. (a) Pristine and annealed SWCNTs, (b) SWCNT film with oxidized PCAT, (c) same sample after reduction of PCAT, (d) same sample after re-oxidation of PCAT, (e) same sample after re-reduction of PCAT, (f) same sample, PCAT oxidized again, and (g) same sample, PCAT reduced again. (h) Pristine and annealed SWCNTs, (i)

SWCNT film with oxidized DPPD, (j) same sample after reduction of DPPD, (k) same sample after re-oxidation of DPPD, (l) same sample after re-reduction of DPPD, (m) same sample, DPPD oxidized again, and (n) same sample, DPPD reduced again.

An analogous experiment to what was just described for the PCAT - SWCNT complex was also conducted using DPPD. (Figs. 6h-n) The shift in the D* peak of the SWCNT Raman spectrum is comparable to the case of PCAT, the same redox agents were used, and the result after three complete redox cycles is identical, again demonstrating the robustness of the effect even for the case of the smaller molecule, which could have been thought to be more prone to removal from the SWCNT network due to its smaller size and hence lesser interaction with the SWCNT surface. If any switchable dopant molecules had been removed from the SWCNT films, however, we would have expected permanent doping due to the sulfate species of the oxidizing agent to occur in those vacancies, as documented in Fig. 2. Additional evidence for the robustness of the interactions of all oxidation states of the switchable dopant aniline oligomers with the SWCNT films comes from rinsing experiments.

3.4. Oligoaniline-SWCNT complexes are robust

In two separate experiments, oxidized DPPD and PCAT molecules respectively were added to a methanolic suspension of SWCNTs and sonicated for one hour. The strongly colored solutions were filtered through PTFE membranes to form coherent nanotube films (“Bucky paper”), which were then rinsed with methanol until the filtrate turned colorless. Raman spectra were taken of these samples before and after further rinsing with several hundred milliliters of methanol, (Fig. 7) indicating that the doping effect is still present after rinsing, and hence the DPPD-SWCNT and

PCAT-SWCNT complexes are stable to rinsing, permitting the manufacture of long term stable devices.

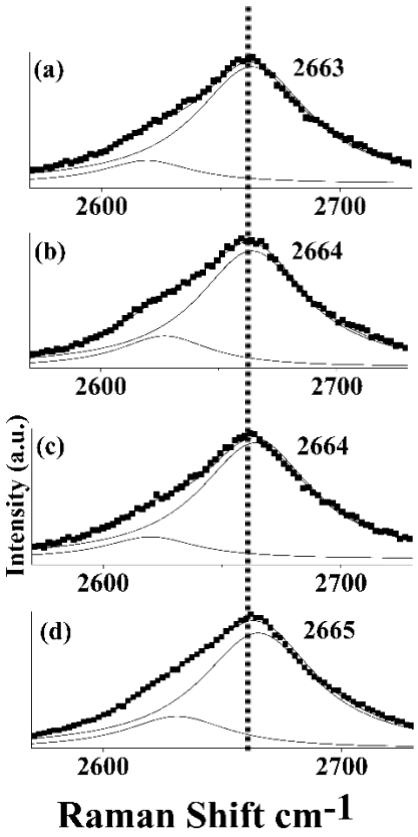

Fig. 7. Stability of SWCNT-oligoaniline complexes towards rinsing with methanol. Raman spectra of SWCNT films (D* peak) (a) with oxidized PCAT before rinsing, (b) with oxidized PCAT after rinsing, (c) with oxidized DPPD before rinsing, and (d) with oxidized DPPD after rinsing.

These complexes are also stable towards the exposure to other potential dopants, such as sulfate SO_4^{2-}. Sulfate ions have been documented as having a strong doping effect of SWCNT networks [34], yet in the case of DPPD-SWCNT and PCAT-SWCNT complexes no lasting effect due to sulfate doping can be detected. Exposure to sulfate is unavoidable during our procedures since it is a product of the oxidation reaction of the oligoanilines with ammonium persulfate. If sulfate could displace the oligoanilines from the SWCNTs, or even co-adsorb onto the SWCNT networks

alongside the oligoanilines, it would have been expected that the p-doping of the SWCNTs could not be reset simply by reducing the oligoanilines. Rather, the SWCNTs would be permanently doped after the first oxidation procedure. This is not the case here, and hence we can state that the oligoaniline-SWCNT complexes are very robust against contamination, which is essential for sensing applications.

3.5. Salt-base conversion of the oligoanilines affects doping

It has been noted in the literature that polyaniline films (and hence also oligoanilines) can themselves be doped by reacting them with an acid (e.g. hydrochloric acid) to form a salt [58,59]. While so far we have presented data from the free base forms of the oxidized and reduced oligoanilines, we will now look at the effect of salt formation. It is desirable to avoid direct doping due to the selected anions, which is why chloride was chosen (as opposed to e.g. sulfate) [36]. While hydrochloric acid has in the past been reported to dope SWCNTs [17], we have shown in previous work that the effect was either due to formation of $FeCl_3$ or due to doping by molecular oxygen formed during sonication in water [35,36]. Here we consider the effect of HCl and KOH in methanolic solution on the doping state of carbon nanotubes in SWCNT-oligonaniline complexes.

Figures 8a-e present a complete cycle of chemical treatments by consecutive rinsing of the DPPD-SWCNT film with ascorbic acid (a reducing reagent), ammonium persulfate (an oxidizing reagent), hydrochloric acid, ascorbic acid, and potassium hydroxide methanolic solutions, while Figs. 8f-j show a different order of treatment of a DPPD-SWCNT sample, namely, ascorbic acid, hydrochloric acid, ammonium persulfate, potassium hydroxide and ascorbic acid. By comparing the outcomes of the two cycles we can separate the effects of salt formation and oxidation from

each other and elucidate the doping properties of all four species (oxidized base, oxidized salt, reduced base, reduced salt).

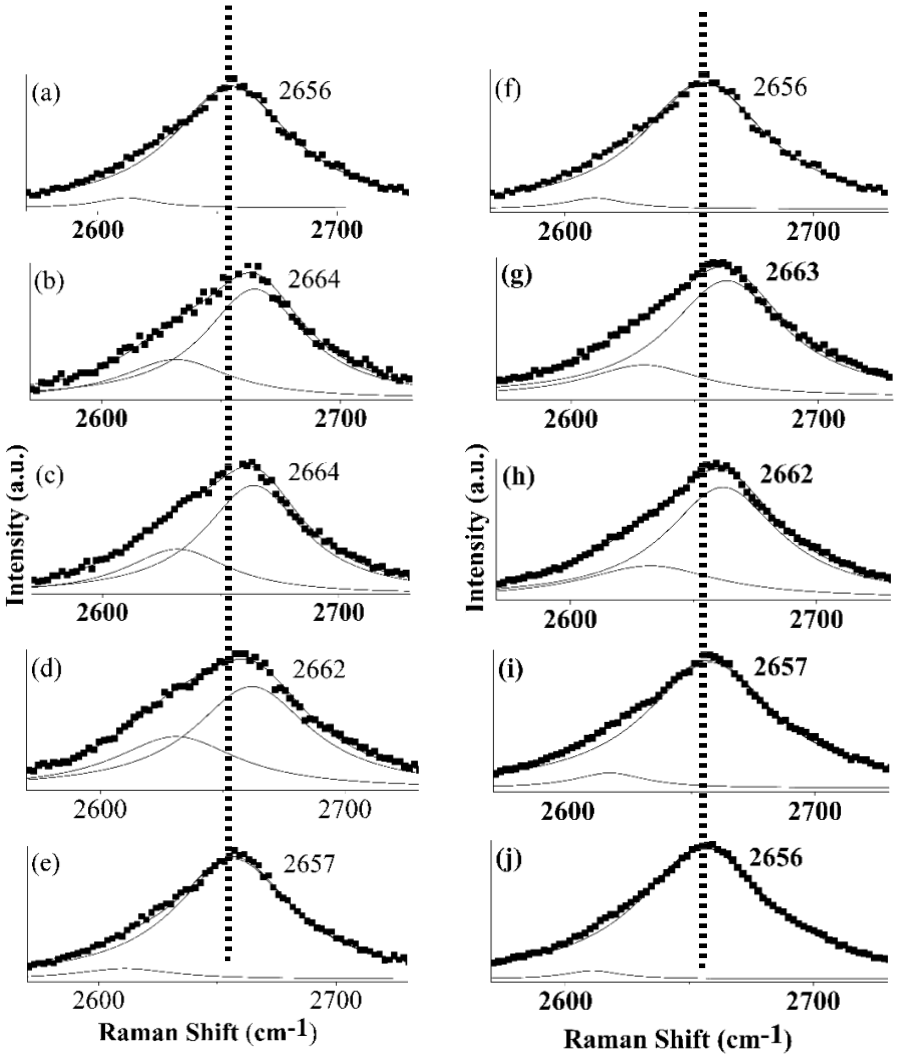

Fig. 8. Acid and base treatment of DPPD/ SWCNT. Raman spectra demonstrating the consecutive chemical treatments of DPPD-SWCNT films. A DPPD-SWCNT film sample was (a) rinsed with ascorbic acid, (b) then rinsed with ammonium persulfate, (c) then rinsed with dilute HCl, (d) then rinsed with ascorbic acid, and (e) finally rinsed with dilute KOH. A different DPPD-SWCNT film sample was (f) rinsed with ascorbic acid, (g) then rinsed with dilute HCl, (h) then rinsed with ammonium persulfate, (i) then rinsed with dilute KOH, and finally (j) rinsed with ascorbic acid.

For the purpose of obtaining the data presented in Fig. 8, DPPD was dissolved in methanol, and SWCNTs were suspended in this solution via sonication for 30 minutes. The solution was then filtered onto a PTFE membrane to form a DPPD-SWCNT film. The film was rinsed with ascorbic acid solution. The Raman spectrum shows a D* peak at 2656 cm^{-1} (Fig. 8a), corresponding to undoped SWCNT networks. The DPPD-SWCNT film was then rinsed with a methanolic ammonium persulfate solution and the Raman spectrum shows a 8 cm^{-1} blue shift of the D* peak to 2664 cm^{-1} (Fig. 8b) attributable to p-doping of the SWCNT networks. Subsequent rinsing with hydrochloric acid solution results in DPPD-SWCNT films with a D* peak at 2664 cm^{-1} (Fig. 8c), still corresponding to p-doping. When the film was rinsed with reducing reagent, it shows a nearly identical D* value at 2662 cm^{-1} (Fig. 8d). It is noteworthy that the oxidized DPPD hydrochloride salt transformed into the reduced DPPD hydrochloride salt, which also p-dopes the SWCNT networks. The final rinsing of the DPPD-SWCNT film with KOH solution results in a down shift of the Raman D* mode back to 2657 cm^{-1} (Fig. 8e). This down shift indicates that the KOH reacted with the reduced DPPD salts back to the reduced DPPD base form which is unable to p-dope the SWCNT networks. In order to ensure that we have properly separated the effects of oxidation state and salt/base form of the DPPD molecules on their ability to p-dope the SWCNT networks, we also subjected a sample to a different cycle, as shown in Figs. 8f-j. This new film was rinsed with reducing reagent solution, resulting in a D* peak at 2656 cm^{-1} (Fig. 8f), corresponding to undoped SWCNT networks. Subsequently, the HCl rinsed DPPD-SWCNT film shows a 9 cm^{-1} blue shift (Fig. 8g) of the Raman D* peak, indicating that reduced DPPD salts accept charge causing SWCNT networks to be p-doped. After rinsing with oxidizing agent, the DPPD-SWCNT film showed no further shift in the D* peak (Fig. 8h) because the reduced DPPD hydrochloride salt turned into oxidized DPPD hydrochloride salt, which also causes p-type doping of the SWCNT

networks. The subsequent rinsing of DPPD-SWCNT networks film with KOH solution results in a red shift of the D* peak found at 2657 cm^{-1} (Fig. 8i). Since this already corresponds to the original state of the SWCNT networks, no further shift is observed after the final rinse with ascorbic acid (Fig. 8j).

It has previously been documented in the literature that protonation of polyaniline by acids preferably occurs at the imine groups of the oxidized species, and enhances the charge transfer from the nanotubes due to the positive charge at the nitrogen centre resulting from protonation [55]. This is consistent with our findings that both the salt and the free base of the oxidized form of DPPD p-dope carbon nanotube films, although the extent of doping observed in our case is identical, likely because the maximum possible charge transfer had already been achieved before protonation. Unlike polyaniline, DPPD does not have intermediate oxidation states, and the preference of protons to attach to imine groups over amine groups does not play a role in our case. Proton attachment to the amine groups in the reduced form of DPPD enhances the charge transfer regardless and leads by itself to p-doping. The free base form of reduced DPPD, as expected, does not p-dope.

A curious effect is observed in Fig. 8i, where the rinsing step with base results in conversion of the DPPD into a species that we have to conclude is the free base of the reduced form. The explanation can be found in the detail of the solvent. In order to exclude doping effects from molecular oxygen that is commonly present in aqueous solutions [36], we have used methanol as a solvent throughout this study. A basic solution of methanol is a known reducing agent, forming formaldehyde in the process. This explains the observed anomaly which we therefore would not expect to be present in aqueous solution.

PCAT exhibits identical behavior when exposed to sequential variations of pH and redox conditions. The data essentially replicates what is shown in Fig. 8 and is presented as Fig. S4 in the supporting material. Hence the behavior is likely generalizable for all aniline oligomers and polyaniline alike. Furthermore, the effect of HCl and KOH on the doping properties of reduced DPPD and PCAT is reproducible and repeatable on the same sample (Supporting material, Fig. S5). Therefore, these systems are also to some extent pH sensitive in addition to being redox-sensitive, an important consideration in sensor design.

3.6. The dopant state can be read electrically

So far, the doping state of the carbon nanotube films was purely determined using Raman spectroscopy, relying on the D* peak shift of a few wavenumbers. In order for the concept of switchable dopants to have any applicability, a more practical read-out is desirable. Indeed, a simple resistivity measurement of the oligoaniline - SWCNT composite films is much more powerful and easy to read (Fig. 9), albeit in itself no proof of doping. The conductivity of a reduced DPPD - SWCNT film is more than doubled upon exposure to a methanolic solution of ammonium persulfate, and could be reset to its original value using a methanolic solution of ascorbic acid (starting at 1200 seconds in Fig. 9). The magnitude of the response is due to the impact that p-dopants generally have on the electronic properties of the host material. Hence the switchable dopant concept can yield simple and robust devices that do not require additional signal amplification, but rather can be based on simple conductivity measurements. Our two-probe set-up here simply employed a power supply and a current meter, but could be further enhanced in bridge configuration or further optimization of the detection circuit. That reliable and reproducible

sensing performance of microfluidic devices built on this principle is indeed achievable even in aqueous medium has been demonstrated by us and was reported separately [56].

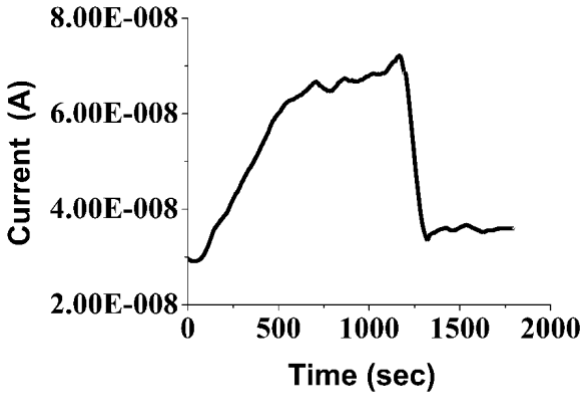

Fig. 9. Current increases during the flow of methanolic ammonium persulfate solution across a DPPD/SWCNT film (0 -1200 sec). Subsequent exposure to a methanolic solution of ascorbic acid (at 1200 sec) results in a rapid decrease in current.

4. Conclusions

We have developed a new concept in nanocarbon doping, which is the utilization of molecules that can respond to chemical stimuli, including, but not limited to, redox reagents and pH as dopants for nanocarbon films. The common characteristic of these molecules is that in response to the given stimulus they reversibly transform between forms that cause clearly distinct doping states of their nanocarbon film hosts. As a result, the presence or absence of the chemical stimulus in question can be detected by determining the doping state of the nanocarbon film, e.g. by Raman spectroscopy or by simple electrical resistance measurements.

In this work, we have demonstrated the concept using two different aniline oligomers (DPPD dimer, PCAT tetramer) in interaction with SWCNT films that are responsive to reduction by

ascorbic acid, oxidation by ammonium persulfate, acidification (salt formation) by HCl and basification (free base formation) by KOH. The charge transfer mechanism is consistent with literature reports [7,55] and was further supported with Raman and XPS spectroscopic studies. The robustness and reproducibility of the switching process was demonstrated.

The basic idea that we have documented here can be further expanded upon by applying it to different forms of nanocarbon, other switchable dopant molecules, analytes and solvents [46,56,57]. At this point, all evidence points toward longterm stability and reproducibility of the systems examined by us. The switchable doping concept further has the significant benefit of not requiring additional amplification such as field effect transistor (ChemFET [12]) geometries, although it may be interesting to examine the potential benefits of combining it with other sensor designs.

Supplementary material

See supplementary material for Raman spectra from additional experiments.

Acknowledgements

We are grateful to Jim Garrett for help with annealing SWCNTs, Steve Kornic for help with Raman spectroscopy, P. Ravi Selvaganapathy and Leo (Huan-Hsuan) Hsu (all McMaster University) for help with the electrical measurements, and Mark Biesinger (Surface Science Western) for help with XPS. The work was financially supported by the Natural Science and Engineering Research Council of Canada through the Discovery Grant program.

References

[1] S. Singh, P. Kruse, Carbon nanotube surface science, Int. J. Nanotechnol. 5 (2008) 900-929.

[2] M.S. Strano, C.A. Dyke, M.L. Usrey, P.W. Barone, M.J. Allen, H. Shan, C. Kittrell, R.H. Hauge, J.M. Tour, R.E. Smalley, Electronic structure control of single-walled carbon nanotube functionalization, Science 301 (2003) 1519-1522.

[3] B.R. Goldsmith, J.G. Coroneus, V.R. Khalap, A.A. Kane, G.A. Weiss, P.G. Collins, Conductance-controlled point functionalization of single-walled carbon nanotubes, Science 315 (2007) 77–81.

[4] J. Kong, N.R. Franklin, C. Zhou, M.G. Chapline, S. Peng, K. Cho, H. Dai, Nanotube molecular wires as chemical sensors, Science 287 (2000) 622-625.

[5] X. Li, L.M. Guard, J. Jiang, K. Sakimoto, J.S. Huang, J. Wu, J. Li, L. Yu, R. Rokhrel, G.W. Brudvig, S. Ismail-Beigi, N. Hazari, A.D. Taylor, Controlled doping of carbon nanotubes with metallocenes for application in hybrid carbon nanotube/Si solar cells, Nano Lett. 14 (2014) 3388-3394.

[6] N. Sinha, J. Ma, J.T.W. Yeow, Carbon nanotube-based sensors, J. Nanosci. Nanotechnol. 6 (2006) 573-590.

[7] C. Klinke, J. Chen, A. Afzali, P. Avouris, Charge transfer induced polarity switching in carbon nanotube transistors, Nano Lett. 5 (2005) 555-558.

[8] E. Akbari, V.K. Arora, A. Enzevaee, M.T. Ahmadi, M. Saeidmanesh, M. Khaledian, H. Karimi, R. Yusof, An analytical approach to evaluate the performance of graphene and carbon nanotubes for NH_3 gas sensor applications, Beilstein J. Nanotechnol. 5 (2014) 726-734.

[9] P. Avouris, Molecular electronics with carbon nanotubes, Acc. Chem. Res. 35 (2002) 1026-1034.

[10] A. Zabet-Khosousi, P.E. Trudeau, Y. Suganuma, A.A. Dhirani, Metal to insulator transition in films of molecularly linked gold nanoparticles, Phys. Rev. Lett. 96 (2006) 156403.

[11] A.W. Snow, F.K. Perkins, M.G. Ancona, J.T. Robinson, E.S. Snow, E.E. Foos, Disordered nanomaterials for chemoelectric vapor sensing: A review, IEEE Sens. J. 15 (2015) 1301-1320.

[12] K. Chikkadi, M. Mouth, C. Roman, M. Haluska, C. Hierold, Advances in NO_2 sensing with individual single-walled carbon nanotube transistors, Beilstein J. Nanotechnol. 5 (2014) 2179-2191.

[13] S. Srivastava, S.S. Sharma, S. Agrawal, S. Kumar, M. Singh, Y.K. Vijay, Study of chemiresistor type CNT doped polyaniline gas sensor, Synth. Met. 160 (2010) 529-534.

[14] C.L. Pint, Z. Sun, S. Moghazy, Y.Q. Xu, J.M. Tour, R.H. Hauge, Supergrowth of nitrogen-doped single-walled carbon nanotube arrays: Active species, dopant characterization, and doped/undoped heterojunctions, ACS Nano 5 (2011) 6925-6934.

[15] U. Dettlaff-Weglikowska, V. Skakalova, R. Graupner, S.H. Jhang, B.H. Kim, H.J. Lee, L. Ley, Y.W. Park, S. Berber, D. Tomanek, S. Roth, Effect of $SOCl_2$ treatment on electrical and mechanical properties of single-wall carbon nanotube networks, J. Am. Chem. Soc. 127 (2005) 5125-5131.

[16] M.D. Ellison, M. Chorney, Reaction of folic acid with single-walled carbon nanotubes, Surf. Sci. 652 (2016) 300-303.

[17] P.G. Collins, K. Bradley, M. Ishigami, A. Zettl, Extreme oxygen sensitivity of electronic properties of carbon nanotubes, Science 287 (2000) 1801-1804.

[18] X. Liu, T. Pichler, M. Knupfer, J. Fink, H. Kataura, Electronic properties of $FeCl_3$-intercalated single-wall carbon nanotubes, Phys. Rev. B 70 (2004) 205405.

[19] J. Lu, S. Nagase, D. Yu, H. Ye, R. Han, Z. Gao, S. Zhang, L. Peng, Amphoteric and controllable doping of carbon nanotubes by encapsulation of organic and organometallic molecules, Phys. Rev. Lett. 93 (2004) 116804.

[20] T. Takenobu, T. Takano, M. Shiraishi, Y. Murakami, M. Ata, H. Kataura, Y. Achiba, Y. Iwasa, Stable and controlled amphoteric doping by encapsulation of organic molecules inside carbon nanotubes, Nat. Mater. 2003, 2, 683–688.

[21] S. Kazaoui, Y. Guo, W. Zhu, Y. Kim, N. Minami, Optical absorption spectroscopy of single-wall carbon nanotubes doped with a TCNQ derivative, Synth. Met. 135-136 (2003) 753-754.

[22] J. Kong, H. Dai, Full and modulated chemical gating of individual carbon nanotubes by organic amine compounds, J. Phys. Chem. B 105 (2001) 2890–2893.

[23] R.J. Chen, Y. Zhang, D. Wang, H. Dai, Noncovalent sidewall functionalization of single-walled carbon nanotubes for protein immobilization, J. Am. Chem. Soc. 123 (2001) 3838-3839.

[23] A. Claye, S. Rahman, J.E. Fischer, A. Sirenko, G.U. Sumanasekera, P.C. Eklund, In situ Raman scattering studies of alkali-doped single wall carbon nanotubes, Chem. Phys. Lett. 333 (2001) 16-22.

[25] H. I. Wang, M.L. Braatz, N. Richter, K.J. Tielrooij, Z. Mics, H. Lu, N.E. Weber, K. Müllen, D. Turchinovich, M. Kläui, M. Bonn, Reversible photochemical control of doping levels in supported graphene, J. Phys. Chem. C 121 (2017) 4083-4091.

[26] K.K. Kim, S.M. Kim, Y.H. Lee, Chemically conjugated carbon nanotubes and graphene for carrier modulation, Acc. Chem. Res. 49 (2016) 390-399.

[27] W. Fu, L. Jiang, E.P. van Geest, L.M.C. Lima, G.F. Schneider, Sensing at the surface of graphene filed-effect transistors, Adv. Mater. 29 (2017) 1603610.

[28] A.L. Ng, C.F. Chen, H. Kwon, Z. Peng, C.S. Lee, Y.H. Wang, Chemical gating of a synthetic tube-in-a-tube semiconductor, J. Am. Chem. Soc. 139 (2017) 3045-3051.

[29] G.M.D. Nascimento, P. Corio, R.W. Novickis, M.L.A. Temperini, M.S. Dresselhaus, Synthesis and characterization of single-wall-carbon-nanotube-doped emeraldine salt and base polyaniline nanocomposites, J. Polym. Sci., Part A: Polym. Chem. 43 (2005) 815-822.

[30] M. Baibarac, I. Baltog, S. Lefrant, J.Y. Mevellec, O. Chauvet, Polyaniline and carbon nanotubes based composites containing whole units and fragments of nanotubes, Chem. Mater. 15 (2003) 4149-4156.

[31] H. Zengin, W. Zhou, J. Jin, R. Czerw, D.W. Smith Jr, L. Echegoyen, D.L. Carroll, S.H. Foulger, J. Ballato, Carbon nanotube doped polyaniline, Adv. Mater. 14 (2002) 1480-1483.

[32] J.E. Albuquerque, L.H.C. Mattoso, D.T. Balogh, R.M. Faria, J.G. Masters, A.G. MacDiarmid, A simple method to estimate the oxidation state of polyanilines, Synth. Met. 113 (2000) 19-22.

[33] W.E. Ford, D. Gao, F. Scholz, G. Nelles, F. von Wrochem, Resistive switching of tetraaniline films: From ultrathin monolayers to robust polymeric blends, Chem. Mater. 25 (2013) 3603-3613.

[34] M.T. Greiner, M. Festin, P. Kruse, Investigation of corrosion-inhibiting aniline oligomer thin films on iron using photoelectron spectroscopy, J. Phys. Chem. C 112 (2008) 18991-19004.

[35] K.R. Moonoosawmy, P. Kruse, To dope or not to dope: The effect of sonicating single-wall carbon nanotubes in common laboratory solvents on their electronic structure, J. Am. Chem. Soc. 130 (2008) 13417-13424.

[36] K.R. Moonoosawmy, P. Kruse, Cause and consequence of carbon nanotube doping in water and aqueous media, J. Am. Chem. Soc. 132 (2010) 1572-1577.

[37] W. Wang, A.G. MacDiarmid, New synthesis of phenyl/phenyl end-capped tetraaniline in the leucoemeraldine and emeraldine oxidation states, Synth. Met. 129 (2002) 199-205.

[38] K.R. Moonoosawmy, P. Kruse, Ambiguity in the characterization of chemically modified single-walled carbon nanotubes: A Raman and ultraviolet-visible-near-infrared study, J. Phys. Chem. C 113 (2009) 5133-5140.

[39] C. Thomsen, Second-order Raman spectra of single and multiwalled carbon nanotubes. Phys. Rev. B 61 (2000) 4542-4544.

[40] A. Das, A.K. Sood, Renormalization of the phonon spectrum in semiconducting single-walled carbon nanotubes studied by Raman spectroscopy, Phys. Rev. B 79 (2009) 235429.

[41] A. Mohtasebi, T. Chowdhury, L.H.H. Hsu, M.C. Biesinger, P. Kruse, P. Interfacial charge transfer between phenyl-capped aniline tetramer films and iron oxide surfaces, J. Phys. Chem. C 120 (2016) 29248-29263.

[42] T. Chowdhury, A. Mohtasebi, S. Kostina, X. Zhang, J.R. Kish, and P. Kruse, Interactions of different redox states of phenyl-capped aniline tetramers with iron oxide surfaces and consequences for corrosion inhibition, J. Electrochem. Soc. 164 (2017) C1013-C1026.

[43] P. Corio, P.S. Santos, V.W. Brar, G.G. Samsonidze, S.G. Chou, M.S. Dresselhaus, Potential dependent surface Raman spectroscopy of single wall carbon nanotube films on platinum electrodes, Chem. Phys. Lett. 370 (2003) 675–682.

[44] T. Chowdhury, E. Hoque, A. Mohtasebi, and P. Kruse, Nature of the interaction of N,N'-diphenyl-1,4-phenylenediamine with iron oxide surfaces, J. Phys. Chem. C 121 (2017) 2721-2729.

[45] T. Chowdhury, A. Mohtasebi, and P. Kruse, Nature of the interaction of N,N'-diphenyl-1,4-benzoquinonediimine with iron oxide surfaces and its mobility on the same surfaces, J. Phys. Chem. C 121 (2017) 2294-2302.

[46] A. Mohtasebi, A.D. Broomfield, T. Chowdhury, P.R. Selvaganapathy, and P. Kruse, Reagent-Free Quantification of Aqueous Free Chlorine via Electrical Readout of Colorimetrically Functionalized Pencil Lines, ACS Appl. Mater. Interfaces 9 (2017) 20748-20761.

[47] L. Ruan, P.R. Norton, W.K. Wan, STM studies of adsorbed ZDDP on graphite, Tribol. Lett. 2 (1996) 189-197.

[48] J. Mathew, S. Emin, E. Pavlica, M. Valant, G. Bratina, Interface-controlled growth of organic semiconductors on graphene, Surf. Sci. 664 (2017) 16-20.

[49] C. Thomsen, S. Reich, J. Maultzsch, Resonant Raman spectroscopy of nanotubes, Philos. Trans. R. Soc. A 362 (2004) 2271-2288.

[50] S.M. Tadayyon, H.M. Grandin, K. Griffiths, P.R. Norton, H. Aziz, Z.D. Popovic, CuPc buffer layer role in OLED performance: a study of the interfacial band energies, Org. Electron. 5 (2004) 157-166.

[51] H.D. Santa, S. Quillard, E. Fayad, G. Louarn, In situ UV-vis and Raman spectroscopic studies of the electrochemical behavior of N,N'-diphenyl-1,4-phenylenediamine, Synth. Met. 156 (2006) 81-85.

[52] C.B. Duke, E.M. Conwell, A. Paton, Localized molecular excitons in polyaniline, Chem. Phys. Lett. 131 (1986) 82-86.

[53] Y. Xia, D.L. Wise, G.E. Wnek, D.J. Trantolo, T.M. Cooper, J.D. Gresser, Electrical and optical polymer systems: Fundamentals, methods and applications, Marcel Dekker: New York, 1998; p. 366.

[54] K.L. Tan, B.T.G. Tan, E.T. Kang, K.G. Neoh, X-ray photoelectron spectroscopy studies of the chemical structure of polyaniline, Phys. Rev. B 39 (1989) 8070-8073.

[55] R.X. Wang, L.F. Huang, X.Y. Tian, Understanding the protonation of polyaniline and polyaniline-graphene interaction, J. Phys. Chem. C 116 (2012) 13120-13126.

[56] L.H.H. Hsu, E. Hoque, P. Kruse, P.R. Selvaganapathy, A carbon nanotube based resettable sensor for measuring free chlorine in drinking water. Appl. Phys. Lett. 106 (2015) 063102.

[57] E. Hoque, L.H.H. Hsu, A. Aryasomayajula, P.R. Selvaganapathy, and P. Kruse, Pencil-Drawn Chemiresistive Sensor for Free Chlorine in Water, IEEE Sens. Lett. 1 (2017) 4500504.

[58] J.N. Barisci, T.W. Lewis, G.M. Spinks, C.O. Too, G.G. Wallace, Conducting polymers as a basis for responsive materials systems. J. Intel. Mater. Syst. Str. 9 (1998) 723-731.

[59] M. Kendig, M. Hon, L. Warren, 'Smart' corrosion inhibiting coatings, Prog. Org. Coat. 47 (2003) 183-189.